PHYSICAL REVIEW C VOLUME 23, NUMBER 5 MAY 1981

# Positive- and negative-parity level structures of $^{194}$Pt from $(n,n'\gamma)$ reaction spectroscopy

A. J. Filo* and S. W. Yates
*Department of Chemistry, University of Kentucky, Lexington, Kentucky 40506*

D. F. Coope,† J. L. Weil, and M. T. McEllistrem
*Department of Physics and Astronomy, University of Kentucky, Lexington, Kentucky 40506*

(Received 6 October 1980)

Energy levels of $^{194}$Pt populated by the $(n,n'\gamma)$ reaction have been studied at incident neutron energies up to 4.5 MeV. Detailed $\gamma$-ray excitation functions were measured between 1.4 and 2.5 MeV, and $\gamma$-ray angular distributions were obtained at 2.5 MeV. Essentially all previously known levels below 2.0 MeV having $J \leq 6$ were observed. New level placements and spins for some previously unassigned levels have been deduced. The negative-parity states with spins from $1^-$ to $6^-$ are interpreted in terms of the semi-decoupled model. The positive-parity states are compared to several models, including the boson expansion theory and the interacting boson model. The interacting boson model adequately accounts for the observed branching ratios, with the exception of the previously noted anomalous 1547-keV $0^+$ state. The boson expansion theory enjoys comparable success for $^{194}$Pt.

[NUCLEAR REACTIONS $^{194}$Pt$(n,n'\gamma)$, $E_n=1.2$–$4.5$ MeV. Measured $E_\gamma$, $I_\gamma$, $\sigma(E,E_\gamma,\theta_\gamma)$. $^{194}$Pt deduced levels, branching ratios, $J$, $\pi$. Compared levels and branching ratios to theory. Enriched target, Ge(Li) detector, time-of-flight background suppression.]

## I. INTRODUCTION

The platinum nuclei fall in a region which is characterized as shape transitional because collective excitations of these nuclei exhibit large departures from both the rotational model[1,2] and the vibrational model.[3] Attempts to understand these structural deviations in terms of small corrections to these models have not been satisfactory, but it is clear that an understanding of the collective properties of nuclei in this region is critical to a unified description of nuclear structure. Although it is generally agreed that a prolate to oblate shape change occurs in going from the stable osmium nuclei to the stable platinum nuclei, the role of the $\gamma$ degree of freedom is the subject of considerable contention.[4,5]

Some models of long standing which have been employed to account for the properties of low-lying states include the triaxially deformed rigid rotor,[6] the rotation-vibration model,[7] and the $\gamma$-unstable model.[8] Kumar and Baranger[9,10] performed model computations with the complete Bohr collective Hamiltonian using potential energy surfaces and inertial parameters calculated within the pairing-plus-quadrupole model of residual interactions.[11,12] They have experienced reasonable success in explaining observed quadrupole moments and reduced transition probabilities in this mass region.

A recent resurgence of interest in transitional nuclei has been fostered by the application of boson calculational techniques to this region. Cizewski *et al.*[13] have proposed that the interacting boson model (IBM) of Arima and Iachello[14-25] provides a good description of these nuclei, and suggest that $^{196}$Pt is an excellent example of the O(6) limiting symmetry[21,25] of this model. This symmetry is similar[25] to that of the $\gamma$-unstable model.[8] In addition, Casten and Cizewski[26,27] have found that the introduction of progressive and systematic departures from the O(6) limit of the IBM can account for variations of empirical characteristics throughout the even-mass Os and Pt nuclei, again affirming the validity of the O(6) limit for heavy Pt nuclei. The boson expansion theory (BET) of Kishimoto and Tamura,[28,29] which is fundamentally different from the IBM although also a boson basis state model, has recently been used to describe collective motions in many transitional nuclei with good success.[30-32] More detailed spectroscopic knowledge of the transitional nuclei is required to fully evaluate and test these models.

We have undertaken the investigation of $^{194}$Pt with the $(n,n'\gamma)$ reaction as the initial phase of a larger detailed study of transitional nuclei. The level properties of $^{194}$Pt had been extensively studied and recently compiled[33] from radioactive decay and a number of different nuclear reaction studies, but inelastic neutron scattering is less selective than other reactions and, consequently, leads to the population of a large number of levels. Moreover, this reaction is not restricted to low-spin states or states of a particular parity, while the use of $\gamma$-ray detection preserves good spectroscopic resolution. In conjunction with this study we have also performed neutron detection time-of-flight studies of $^{194}$Pt. Those data, along with the inelastic scattering cross sections deduced from this work, will be presented in a future article.[34]

## II. EXPERIMENTAL PROCEDURES

The techniques employed in these measurements were similar to those of previous $(n,n'\gamma)$ studies in this laboratory.[35-37] The pulsed proton beam from a 6.5-MV Van de Graaff accelerator with a repetition rate of 2 MHz and a pulse width of ~7 ns was focused through a 3.3 $\mu$m molybdenum entrance foil into a tantalum-lined cell containing slightly less than 1 atm of tritium gas. Neutrons were produced by the $^3$H$(p,n)^3$He reaction. The scattering sample of enriched (97.4% $^{194}$Pt) metallic platinum powder with 42 g mass was contained in a cylinder of polyethylene with a diameter of 1.5 cm, a height of 3.0 cm, and a wall thickness of 0.25 mm. This sample was suspended at a distance of 6.3 cm from the end of the gas cell at 0° relative to the beam axis. With these conditions, a typical neutron energy spread of 70 keV was realized at the scattering sample for incident energy ~2 MeV.

A coaxial Ge(Li) detector with an efficiency of 15% for 1.33-MeV $\gamma$ rays (relative to a 7.6 × 7.6 cm NaI(Tl) detector at 25 cm) was positioned approximately 75 cm from the sample on a goniometer. The Ge(Li) detector was shielded from the direct neutron flux by a tungsten shadow bar, while a hollow cylinder of lead surrounded by $Li_2CO_3$ and paraffin was used to shield the detector from the general neutron and photon background. The energy resolution of the detector was 2.2 keV full width at half maximum (FWHM) at 1332 keV. Radioactive sources of $^{152}$Eu and $^{137}$Cs were used as external sources for energy and efficiency calibration of the Ge(Li) detector. These sources were counted in identical geometries and counting (and gating) conditions as those of the actual measurements of $^{194}$Pt. Well-known transitions[38] in $^{194}$Pt were also used for internal energy calibrations. Other internal spectral calibrations were obtained by counting the $^{152}$Eu source simultaneously with the $\gamma$ rays produced by the neutron bombardment of the $^{194}$Pt sample.

For normalization of the individual runs a conventional long counter[39] located perpendicular to the beam axis at a distance of 3 m from the target cell monitored the neutron flux. The usual time-of-flight (TOF) techniques, where the $\gamma$-ray energy spectrum is gated with the prompt photon peak of the time spectrum, were employed to discriminate between prompt $\gamma$ rays and background events in the detector. The signals from the detector were digitized with a 4096-channel analog-to-digital converter (ADC) and stored in a computer memory. A typical $\gamma$-ray spectrum is shown in Fig. 1.

Gamma-ray yields were measured as a function

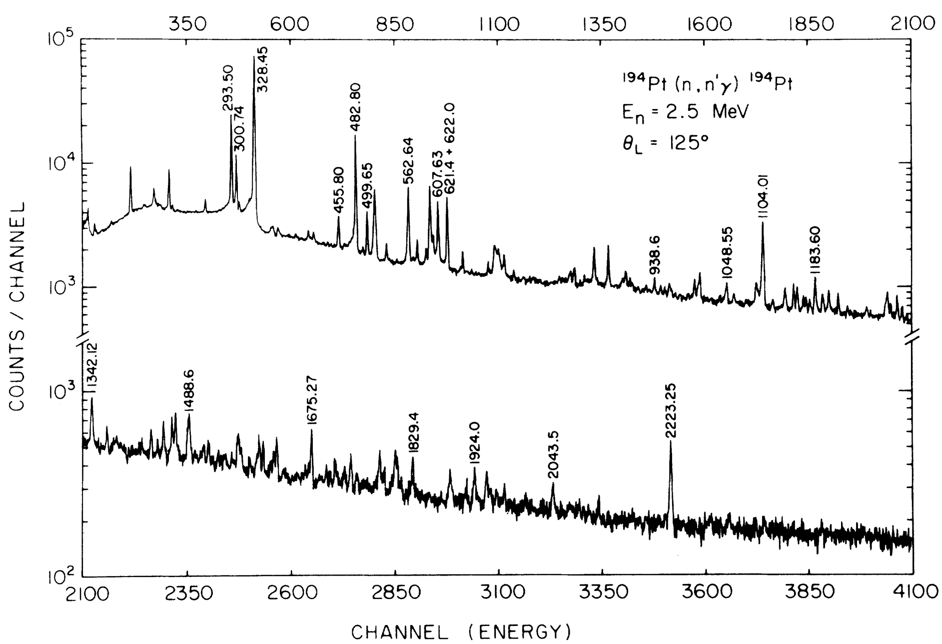


FIG. 1. Spectrum of $\gamma$ rays from 2.5 MeV neutrons incident on $^{194}$Pt. Many of the prominent peaks from $^{194}$Pt $\gamma$ rays are identified by energy in keV.

of incident neutron energy in 50-keV steps from 1.4 to 2.5 MeV and also at 1.2, 3.5, and 4.5 MeV. From these excitation functions the $\gamma$-ray thresholds were deduced. Angular distributions of $\gamma$ rays were measured at $E_n = 2.5$ MeV for 12 angles evenly spaced between 40° and 150° relative to the beam axis.

Background spectra were measured at several energies by substituting an enriched $^{208}$Pb sample in the target position. Since $^{208}$Pb has no excited states below 2.61 MeV, no $\gamma$ rays are produced by scattering low-energy neutrons; otherwise, this sample is similar in density, $Z$, and $A$ to $^{194}$Pt. A search was made for isomeric states having $t_{1/2} > 5$ ns which might be populated by the inelastic scattering reaction, but none were found.

## III. DATA REDUCTION AND RESULTS

The peak fitting program SAMPO (Ref. 40) was used to extract peak centroids and yields. Relative efficiencies for yield corrections were obtained from the efficiency calibration noted above using the piecewise cubic spline procedure described by Conte and deBoor[41] for interpolation. Energies of $\gamma$ rays were obtained from centroids using an energy calibration curve which was a second order polynomial least squares fit to centroids of peaks of known energies.

The large $^{194}$Pt sample required for this work leads to several pernicious effects for which corrections must be employed. The extracted $\gamma$-ray yields must be corrected for sample $\gamma$-ray absorption, neutron attenuation, and multiple elastic and inelastic neutron scattering. Corrections to the data have been made for the effects of $\gamma$-ray absorption with a computer code developed in this laboratory.[42] The analytic expressions of Engelbrecht[43] were used to correct for neutron attenuation and scattering in the cylindrical sample. All $\gamma$-ray yields were compared, for normalization to cross sections, with the well-known cross section[44,45] of the 847-keV $\gamma$ ray of $^{56}$Fe obtained by inelastic scattering from a natural iron sample. Corrections for the yield of this $\gamma$ ray were treated consistently with those for $^{194}$Pt.

### A. Excitation functions

Detailed excitation function measurements were made with the Ge(Li) detector placed at 125° relative to the beam axis to facilitate relating the detector yields to angle integrated cross sections. By extrapolating the $\gamma$-ray yields to threshold, the decaying level can be placed. These threshold values, together with the accurately measured $\gamma$-ray energies, were used to fit transitions into the decay scheme.

A $\gamma$-ray spectrum was also taken at an incident neutron energy of 1.2 MeV in order to measure the branching ratio of decays from the 622-keV second $2^+$ state. At higher energies knowledge of this ratio proved important in separating the contribution of this 622.0-keV transition from that of the 621.4-keV transition from the $3^-$ state at 1432.5 keV. Measurements at 3.5 and 4.5 MeV revealed a surprisingly small number of transitions which were not observed at lower incident neutron energies.

Figures 2 and 3 display examples of $\gamma$-ray excitation functions. When transitions from low-spin ($J \leq 2$) states evince little feeding from higher-lying states, their excitation functions are characterized as rising sharply above threshold, leveling off a few hundred keV above threshold, and (in many cases) then decreasing. At least, the curvature of the energy dependence is always negative. The excitation functions from intermediate-spin ($J = 3$ or 4) states tend to increase nearly linearly, while the slopes of the excitation functions of higher-spin ($J \geq 5$) states always increase, or the curvature is positive, with bombarding energy. The excitation functions can be used, therefore, not only to obtain thresholds and level placements

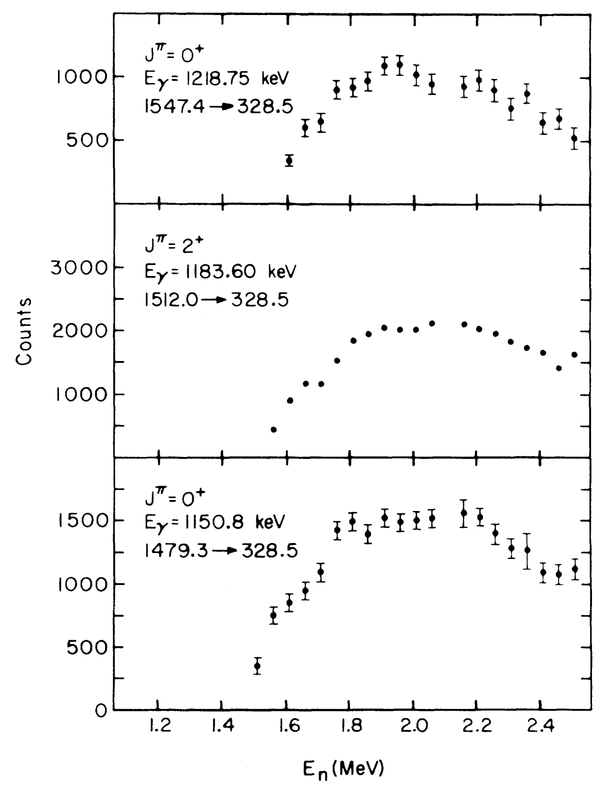


FIG. 2. Excitation functions of $\gamma$ rays from some low-spin states in $^{194}$Pt. The $J^\pi$ given is that of the emitting state.

but also to deduce limits on the transferred angular momentum. This spin-dependent behavior of excitation functions has been noted previously for rare earth nuclei.[46]

The 455.8-keV transition which has also been observed[47,48] in the $^{192}$Os($\alpha$, $2n\gamma$) reaction has been placed as deexciting a new level at 1883.3 keV to the $3^-$ state at 1432.5 keV. The shape of the excitation function indicates that this transition is from a state of intermediate spin, and the fact that it has only been observed previously in the ($\alpha$, $2n\gamma$) reaction adds further support to the suggestion that it is not a low-spin level. Recent reexamination[49] of in-beam $\gamma$-ray measurements, at our suggestion, reveals this transition to be in coincidence with $\gamma$ rays depopulating the $3^-$ state and provides additional confirmation of its placement.

### B. Angular distributions

If the anisotropies of the $\gamma$-ray angular distributions are substantial, it is often possible to deduce unique spin values for the decaying levels or, at least, to limit assignments to a few possibilities.[50] These anisotropies at low incident energies are essentially independent of the neutron scattering mechanism. They depend, however, on the alignment of the excited level produced in the neutron scattering.[50] At energies not too far from threshold, the outgoing neutrons correspond to a few partial waves, and low $m$ magnetic substates are more strongly populated than others. Hence the level alignment is a maximum when the outgoing neutrons are so low in energy that they have only $l=0$ components. An incident energy of 2.5 MeV was selected here to give adequate scattering strength to levels of interest in this study; yet few of these levels were being fed by cascades from higher levels, and this energy was low enough to produce good alignment for states excited.

Yields at each of the 12 angles of measurement were corrected for scattering and absorption effects. Figures 4 and 5 show examples of angular distributions of several transitions. The distinction between dipole and quadrupole transitions is evident, as is the isotropy of the decay of the 1547-keV $0^+$ state.

The yields were fitted with the even-order Le-

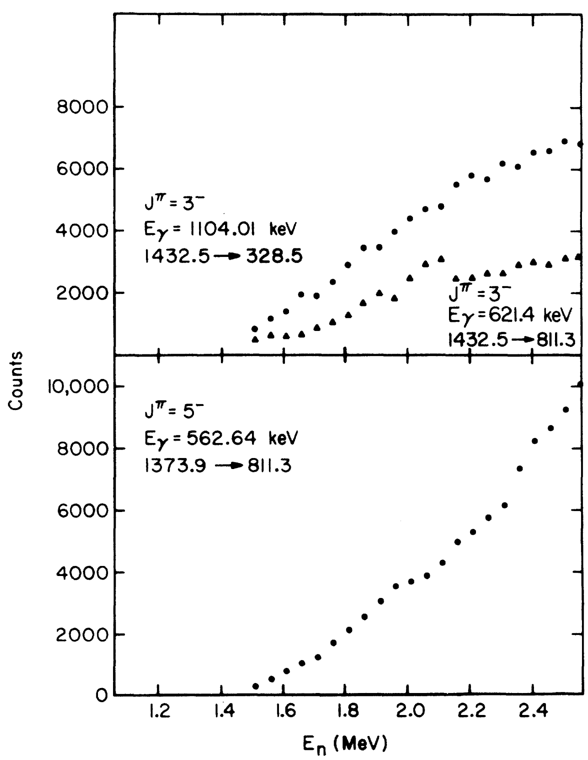


FIG. 3. Excitation functions of the 562.6-, 621.4-, and 1104.0-keV transitions. The $J^\pi$ given is that of the emitting state.

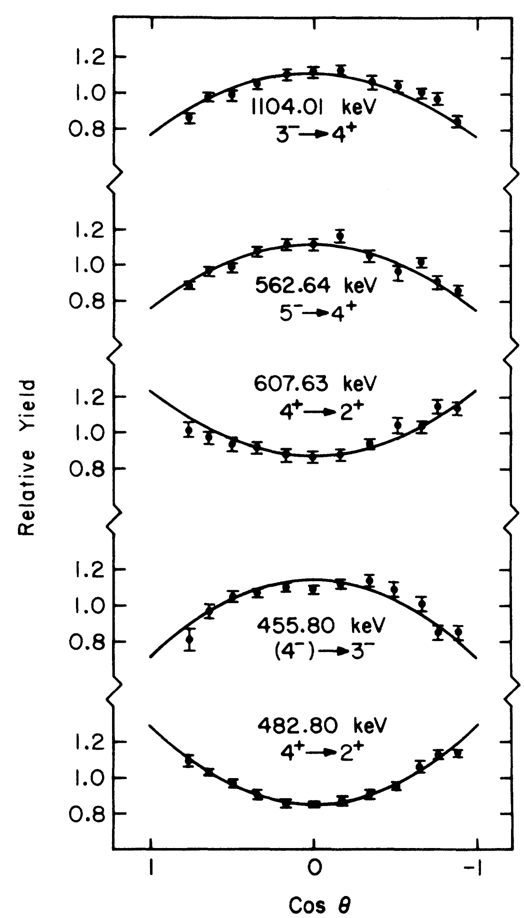


FIG. 4. Angular distributions of some of the $\gamma$ rays from $^{194}$Pt. The solid curves are least-squares Legendre polynomial fits to the relative yields.

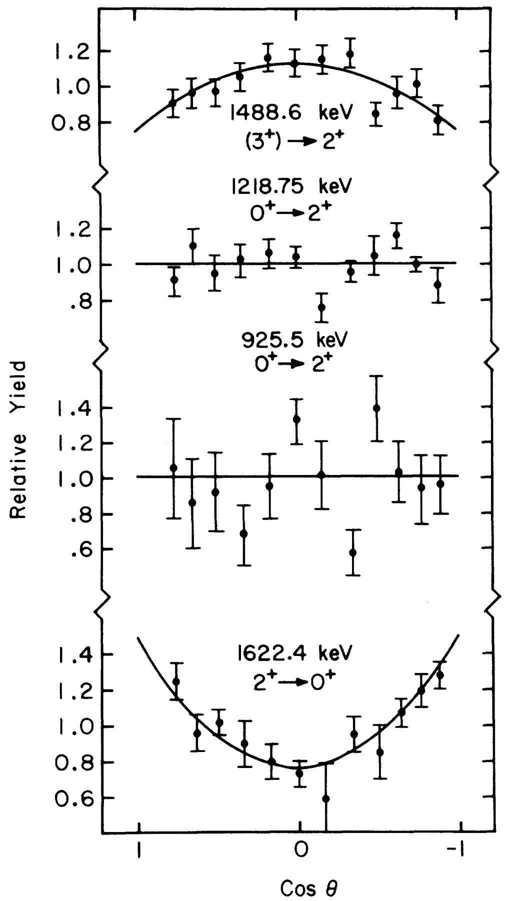


FIG. 5. Angular distributions of some of the $\gamma$ rays from $^{194}$Pt. The solid curves are least-squares Legendre polynomial fits to the relative yields.

gendre polynomial expression

$$Y(\theta)=A_0[1+a_2P_2(\cos\theta)+a_4P_4(\cos\theta)]\,.$$

The solid curves in Figs. 4 and 5 are the fits, while the error bars represent the relative uncertainties of each datum. The order of the coefficients for the fit and uncertainties were determined by a least squares procedure. A chi-square test was applied to each fit and the significance of each additional coefficient was determined by an $F$-test of the chi square. In general, the uncertainties associated with the $a_4$ term exceeded the value of the coefficient; therefore, the $a_4$ terms were ignored in the interpretation. Isotropy was indicated for fits in which the $a_2$ term was rejected. The results of the fits to the angular distribution measurements are contained in Table I.

Interpretation of the anisotropies of Table I could be complicated by cascade feeding of a level, since extensive feeding can destroy the excited state alignment produced by direct excitation in neutron scattering. That this was not the case in this ex-

TABLE I. Energies, intensities, angular distribution coefficients, and transition assignments of $\gamma$ rays observed in the $^{194}$Pt$(n,n'\gamma)$ reaction at $E_n$ = 2.5 MeV.

| Energy[a] (keV) | Relative[b] intensity | $a_2$ | Transition ($E_{\text{initial}} \to E_{\text{final}}$) |
|---|---|---|---|
| 202.8 (2) | 0.8 | | 1433 → 1230 |
| 293.50 (5) | 28.8 | −0.04 (4) | 622 → 328 |
| 300.74 (7) | 10.6 | 0.02 (4) | 923 → 622 |
| 304.8 (3) | 1.1 | | 1817 → 1512 |
| 328.45 (3) | 100 | 0.12 (4) | 328 → 0 |
| 364.8 (2) | 0.59 | | 1797 → 1433 |
| 409.69 (10) | 0.47 | 0.40 (14) | 1784 → 1374 |
| 417.96 (11) | 0.62 | 0.13 (15) | 1230 → 811 |
| 455.80 (9) | 1.9 | −0.28 (3) | 1888 → 1433 |
| 482.80 (6) | 19.0 | 0.29 (2) | 811 → 328 |
| 499.65 (9) | 2.9 | | 1422 → 923 |
| 529.0 (2) | 0.94 | 0.30 (9) | 1961 → 1433 |
| 562.64 (8) | 6.5 | −0.24 (3) | 1374 → 811 |
| 575.9 (2) | 1.1 | 0.33 (9) | 1499 → 923 |
| 589.18 (11) | 0.48 | | 1512 → 923 |
| 594.3 (2) | 1.2 | | 923 → 328 |
| 600.3 (2) | 0.57 | | 1412 → 811 |
| 607.63 (9) | 4.3 | 0.24 (3) | 1230 → 622 |
| 621.4 (2) | 2.2 | | 1433 → 811 |
| 622.0 (2) | 3.5 | | 622 → 0 |
| 645.16 (10) | 0.85 | 0.09 (14) | 1267 → 622 |
| 684.08 (12) | 0.45 | | |
| 700.5 (2) | 0.61 | | 1512 → 811 |
| 810.5 (2) | 0.46 | −0.24 (14) | 1433 → 622 |
| 816.2 (3) | 0.53 | 0.12 (12) | |
| 889.90 (15) | 0.41 | | 1512 → 622 |
| 894.51 (13) | 0.78 | 0.08 (9) | 1817 → 923 |
| 901.05 (17) | 0.31 | | 1230 → 328 |
| 925.5 (3) | 0.34 | 0.08 (22) | 1547 → 622 |
| 938.6 (2) | 0.52 | 0.01 (8) | 1267 → 328 |
| 948.3 (2) | 0.43 | −0.18 (25) | 2215 → 1267 |
| 999.99 (14) | 0.56 | −0.32 (12) | 1622 → 622 |
| 1007.57 (9) | 0.93 | 0.06 (7) | 1930 → 923 |
| 1048.55 (13) | 0.84 | 0.02 (8) | 1671 → 622 |
| 1059.8 (3) | 0.28 | | |
| 1093.9 (2) | 0.68 | 0.34 (12) | 1422 → 328 |
| 1104.01 (8) | 5.9 | −0.23 (3) | 1433 → 328 |
| 1118.7 (3) | 0.28 | | 1930 → 811 |
| 1137.8 (2) | 0.68 | −0.01 (10) | |
| 1150.8 (2) | 0.91 | | 1479 → 328 |
| 1156.5 (2) | 0.81 | 0.10 (5) | 1779 → 622 |
| 1165.6 (2) | 0.57 | | |
| 1169.9 (3) | 0.43 | | |
| 1175.4 (2) | 0.22 | | 1797 → 622 |
| 1183.60 (12) | 1.4 | 0.18 (6) | 1512 → 328 |
| 1194.8 (2) | 0.69 | −0.22 (6) | 1817 → 622 |
| 1218.75 (13) | 0.71 | 0.00 (7) | 1547 → 328 |
| 1293.5 (2) | 0.67 | | 1622 → 328 |
| 1308.3 (2) | 0.76 | −0.29 (13) | 1930 → 622 |
| 1342.12 (14) | 0.90 | −0.18 (12) | 1671 → 328 |
| 1431.6 (3) | 0.32 | 0.08 (9) | 2054 → 622 |
| 1441.6 (3) | 0.29 | | 2064 → 622 |
| 1450.5 (2) | 0.68 | −0.13 (6) | 1779 → 328 |
| 1468.99 (12) | 0.85 | 0.01 (8) | 1797 → 328 |
| 1488.6 (2) | 1.5 | −0.24 (7) | 1817 → 328 |
| 1511.6 (4) | 0.19 | | 2134 → 622 |
| 1518.7 (2) | 0.61 | | 2141 → 622 |

TABLE I. (*Continued*).

| Energy[a] (keV) | Relative[b] intensity | $a_2$ | Transition ($E_{initial} \rightarrow E_{final}$) |
|---|---|---|---|
| 1568.8 (3) | 0.42 | | |
| 1595.6 (2) | 0.57 | | 1924 → 328 |
| 1601.8 (2) | 0.62 | | 1930 → 328 |
| 1622.4 (3) | 0.74 | 0.49 (6) | 1622 → 0 |
| 1675.27 (15) | 0.93 | 0.41 (9) | 2004 → 328 |
| 1715.2 (2) | 0.31 | | 2044 → 328 |
| 1735.2 (2) | 0.47 | | 2064 → 328 |
| 1805.7 (2) | 0.59 | | 2134 → 328 |
| 1829.4 (2) | 0.66 | | 2158 → 328 |
| 1886.6 (2) | 0.61 | | 2215 → 328 |
| 1924.0 (2) | 0.61 | | 1924 → 0 |
| 1969.6 (3) | 0.24 | | 2298 → 328 |
| 2043.5 (2) | 0.63 | | 2044 → 0 |
| 2068.8 (5) | 0.19 | | 2397 → 328 |

[a] Uncertainties in the least significant figures are indicated in parentheses.

[b] Intensities are normalized to 100 for the 328.45-keV $\gamma$ ray.

periment was verified by direct calculation of cascade corrections and is also illustrated by the two "stretched $E2$" transitions in Fig. 4. The 482.8-keV transition from the lowest $4^+$ level at 811.3 keV is fed by six transitions, amounting to 48% of the total intensity. The 607.6-keV transition, a $4^+$ to $2^+$ transition from the 1229.5 keV level, is fed by only one rather weak line, amounting to about 15% of its intensity. Both transitions have the same anisotropy, as is evident in Fig. 4. Even the 48% cascading of the 482.8-keV line has not materially altered its anisotropy.

### C. Level scheme

The level structure of $^{194}$Pt has been previously studied from the $\beta^-$ decay of the $^{194}$Ir isomers, the electron capture decay of $^{194}$Au, and a variety of nuclear reactions, and the results have recently been compiled.[33,38] Such studies have led to a relatively complete characterization of the low-lying states in $^{194}$Pt, and it is perhaps the best described of the platinum nuclei. In the interest of brevity, we will discuss only significant new contributions of this work to the understanding of the level scheme, shown in Fig. 6. We have, of course, confirmed most of the previous placements and assignments, and our $\gamma$-ray intensity values provide accurate branching ratio data for many of these levels.

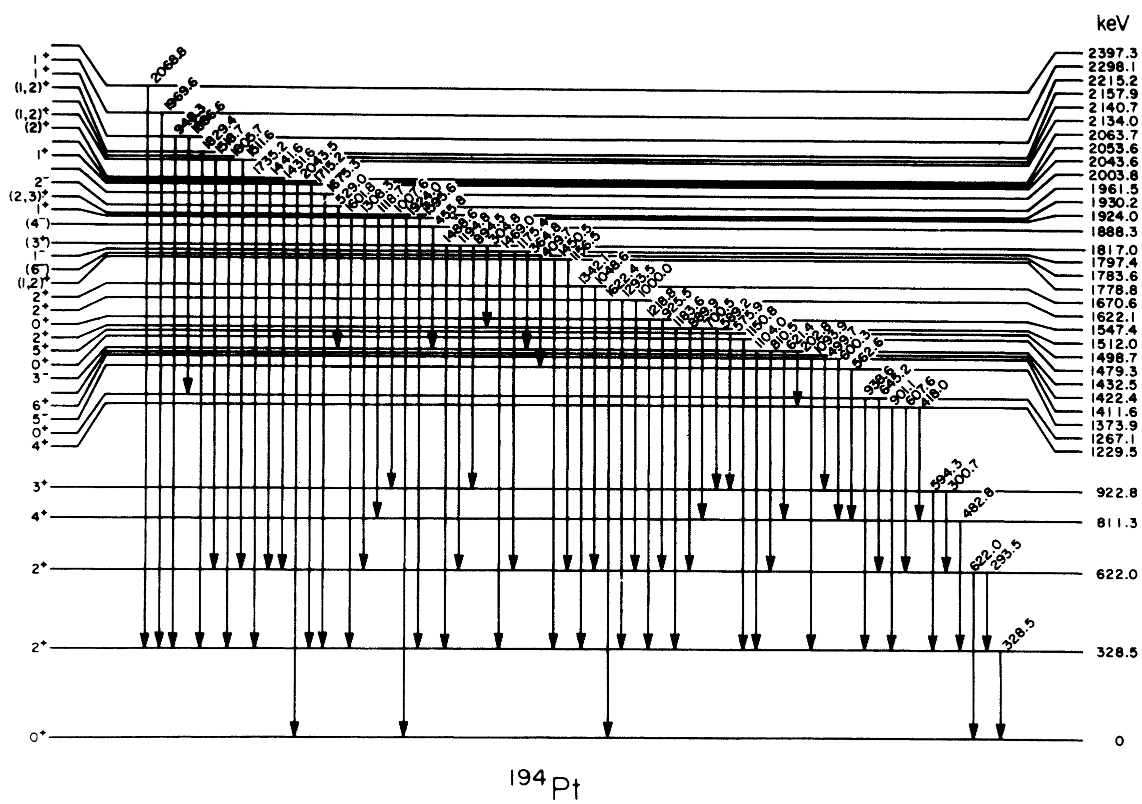


FIG. 6. The level scheme of $^{194}$Pt. The level and $\gamma$-ray energies are in keV, while uncertain assignments are in parentheses.

*1373.9-keV level.* This level decays only to the $4^+$ level at 811.3 keV and had been assigned $J^\pi = (5^-)$ in previous studies.[51,52] It is strongly populated in in-beam $\gamma$-ray measurements.[47,48] The excitation function of its 562.6-keV $\gamma$ ray is consistent only with $J \geq 4$ (see Fig. 3). The anisotropy shown in Fig. 4 is characteristic of that for a dipole transition from a $J=5$ level. Moreover, if $J$ were less than five, the scattering intensity would be greater than we observe. Our results are entirely consistent with earlier suggestions that $J=5$. Accepting also the previous parity assignment, the significance of this level within the framework of the semi-decoupled model will be discussed later.

*1498.7-keV level.* This state decays only to the $3^+$ state at 922.8 keV and has been proposed[48] as the $(5^+)$ member of the quasi-$\gamma$-vibrational band of $^{194}$Pt. The excitation function of the 575.9-keV decay has positive curvature near threshold, indicating $J>3$, while its intensity is too strong for $J>5$. The large anisotropy, $a_2=0.33$, could only be obtained for $J \geq 3$ and is just that of a stretched $E2$ transition from a $J=5$ level. Our data strongly support a $5^+$ assignment.

*1817.0-keV level.* A possible level at this energy was reported[53] from the electron capture decay of $^{194}$Au. There are four transitions, namely the 304.8-, 894.5-, 1194.8-, and 1488.6-keV $\gamma$ rays, which depopulate this level to states with spins of $2^+$ or $3^+$. The angular distribution data show predominantly dipole transitions to two $2^+$ states, and the transition to the $3^+$ state is isotropic. The spin must be 2 or 3, and we have made a tentative $(3^+)$ suggestion based weakly on the absence of transition to the ground state.

*1888.3-keV level.* This new level decays by a 455.8-keV $\gamma$ ray to the $3^-$ state at 1432.5 keV. The angular distribution data (see Fig. 4) suggests that the 455.8-keV $\gamma$ ray is of dipole character, while the nearly linear excitation function of this state indicates a level of intermediate spin. We give this level a $J=4$ assignment. Although a spin of 3 is also possible and the parity is admittedly undetermined, we tentatively suggest $J^\pi = (4^-)$ and include this level with the known negative-parity states in the discussion section. This spin would seem more consistent with the observation of the $\gamma$ ray from this state in the $(\alpha, 2n\gamma)$ reaction.[47-49]

It is noteworthy that a couple of previously reported states below 2 MeV are not populated by the $(n, n'\gamma)$ reaction, which is regarded as reasonably nonselective. A state at 1592.8 keV reported[48] following in-beam $\gamma$-ray studies is not observed in our work. However, more recent studies[49] of $^{194}$Pt do not support this placement and, in conjunction with the present data, we must conclude that the existence of this level is questionable. Another level not noted in our work was proposed[53] at 1803.1 keV, and in this case its absence probably also indicates that the previous placement is incorrect. It appears that all of the remaining $J \leq 6$ levels in $^{194}$Pt are populated by the $(n, n'\gamma)$ reaction. While some $\gamma$-ray branches are not observed, their absence can be ascribed to spectral interferences with background or other sample $\gamma$ rays.

## IV. DISCUSSION

### A. Positive-parity states

As outlined in the Introduction a number of nuclear models have been proposed to explain the low-lying collective excitations in the platinum nuclei. Several of these models have enjoyed some success, and Table II gives a comparison of calculated branching ratios from the quasi-$\gamma$ band for various models with our results. On the basis of this limited presentation it is difficult to argue that one of these descriptions is clearly superior. We will, however, direct our consideration primarily toward an interpretation of $^{194}$Pt in terms

TABLE II. Relative $E2$ transition probabilities for states of the quasi-$\gamma$ band of $^{194}$Pt.

| | $\frac{2_2^+ \to 0_1^+}{2_2^+ \to 2_1^+}$ | $\frac{3_1^+ \to 2_1^+}{3_1^+ \to 2_2^+}$ | $\frac{3_1^+ \to 4_1^+}{3_1^+ \to 2_2^+}$ | $\frac{4_2^+ \to 2_1^+}{4_2^+ \to 2_2^+}$ | $\frac{4_2^+ \to 4_1^+}{4_2^+ \to 2_2^+}$ |
|---|---|---|---|---|---|
| Experiment | 0.003 | 0.004 | 0.70 | 0.010 | 0.94 |
| BET[a] | $<10^{-4}$ | $<10^{-4}$ | 0.35 | 0.007 | 0.80 |
| IBM[b] | $<10^{-4}$ | $<10^{-4}$ | 0.40 | 0 | 0.91 |
| PPQ[c] | 0.002 | 0.003 | 0.40 | | |
| ARM ($\gamma=31.5°$)[d] | 0.012 | 0.015 | 0.54 | 0.037 | 0.56 |
| $\gamma$-unstable[e] | 0 | 0 | 1.05 | 0 | 0.91 |

[a] Boson expansion theory—Ref. 31.
[b] Interacting boson model—Ref. 27.
[c] Pairing-plus-quadrupole model—Ref. 10.
[d] Asymmetric rotor model—Ref. 6.
[e] $\gamma$-unstable model—Refs. 8 and 54.

of the IBM (Refs. 14–25) and BET (Refs. 28 and 29) because of the timeliness of detailed comparisons with these models and the recent successes[26,27,30–32] obtained in this, and other, mass regions with these models.

In the IBM, even-even nuclei are described as a system of interacting bosons which can occupy $L=0$ and $L=2$ ($s$ and $d$) states. These bosons generate an SU(6) symmetry in which three natural limits arise for which analytical solutions are possible. Two of the subgroups of SU(6), SU(5) and SU(3), correspond approximately to the anharmonic vibrator and the axial rotor, respectively, in geometrical terms and are displayed by transitional nuclei in other mass regions[17] and by the well-deformed rare earth nuclei.[22] The third subgroup, O(6), has been suggested[21,25] as a useful description of nuclei at the end of major shells—e.g., the Ba and Pt regions. It has been shown[54] that, for an infinite number of bosons, the O(6) limit corresponds to the $\gamma$-unstable model of Wilets and Jean.[8] While the rigid-triaxial-rotor model[6] (with $\gamma = 30°$) satisfies the same decay selection rules, it differs with respect to $B(E2)$ values and level energies.

The difficulty of deciding about the dynamical character of these nuclei by looking at level energies and decays is illustrated by the results in Table II. Both the IBM and the BET imply $\gamma$-soft or $\gamma$-unstable character. But perhaps as good a representation of the branching ratios is that of the triaxial rigid rotor.[6] Looking in a more complete way at the decays and levels, Cizewski *et al.*[13] showed that $^{196}$Pt is an excellent example of the O(6) limiting symmetry of the IBM. They demonstrated remarkable agreement between the structure of the low-spin positive parity states below the pairing gap and the IBM predictions. All of the low-spin states of the O(6) limit were identified, and excellent agreement with theory was obtained for the $\gamma$-ray branching ratios. Two-neutron transfer strengths in the Pt nuclei have also been shown[55,56] to be consistent with the predictions of the IBM.

Casten and Cizewski[26,27] have found that perturbations from the O(6) limit account for collective properties throughout the even-$A$ Os and Pt nuclei, and have thus examined the O(6) to rotor transition. As part of this study, they evaluated the decay properties of known levels in $^{194}$Pt and found good agreement by assuming $^{194}$Pt to be slightly more perturbed from the O(6) limit than $^{196}$Pt.

An alternative description of collective motions in transitional nuclei is afforded by the boson expansion theory (BET) of Kishimoto and Tamura.[28,29] The BET is microscopic in that it starts with fermions occupying realistic single-particle orbits and then introduces a particle-hole quadrupole-quadrupole interaction and a pairing interaction of both monopole and quadrupole types. The strengths of two residual interactions are the only free parameters of the model and are constrained to have values which vary little from nucleus to nucleus and are near unity. The Hamiltonian is written in a form that is quadratic in fermion pair operators which are then expanded in a series of products of boson operators. The expansion is carried out to sixth order.[30] BET calculations have enjoyed impressive success in the Sm region[30] and have recently been applied to other regions,[31,32] also with good success.

Weeks and Tamura[31] examined collective states in the Os and Pt nuclei in terms of the BET and concluded that the BET describes the features of these nuclei very well. While we will dismiss model comparisons based on level energies, since the IBM calculations[26,27] for $^{194}$Pt did not distinguish between neutron and proton bosons as has recently become possible,[24] both theories provide good agreement with observed branching ratios. Moreover, the BET correctly fits the signs and magnitudes of the static quadrupole moments of the $2_1^+$ states in this region, predicting the Pt nuclei to be oblate in accord with experimental findings.[57–60] In the O(6) limit of the IBM, $Q(2_1^+)=0$ when the proton-neutron degree of freedom is not included.

One of the earliest noted[13] advances of the IBM lies in its explanation of the decay of $0^+$ states and the prediction of $0^+$-$2^+$-$2^+$ triads of excited states. As Table III illustrates, however, the $0_4^+$ state in $^{194}$Pt is anomalous in the IBM. One possible answer[27] could be that the $0_4^+$ state is not a collective state, but the $(p,t)$ reaction data of Deason *et al.*[55] appears to confirm that this is indeed the collective state predicted by the IBM. The BET predictions[31] for $0^+$ excited states are also given in Table III for comparison.

In general the features predicted by both of these models are similar, as seen in part from the

TABLE III. Relative $E2$ transition probabilities for $0^+$ states of $^{194}$Pt.

| | $\frac{0_2^+\to 2_1^+}{0_2^+\to 2_2^+}$ | $\frac{0_3^+\to 2_1^+}{0_3^+\to 2_2^+}$ | $\frac{0_4^+\to 2_1^+}{0_4^+\to 2_2^+}$ | $\frac{0_5^+\to 2_1^+}{0_5^+\to 2_2^+}$ | $\frac{0_6^+\to 2_1^+}{0_6^+\to 2_2^+}$ |
|---|---|---|---|---|---|
| Experiment[a] | 0.09 | 23 | 0.52 | >10 | 0.03 |
| BET[b] | 0.03 | 333 | 0.67 | | |
| IBM[c] | 0 | 17 | 0.003 | 33 | 0 |

[a]Values from radioactive decay data (Ref. 33) were used in cases where the present experimental intensities displayed large uncertainties.

[b] Boson expansion theory—Ref. 31.

[c] Interacting boson model—Ref. 27.

limited comparisons given in Tables II and III. Both models are remarkably successful in this shape-transitional region. The BET does have the special virtue of predicting the quadrupole moments of the $2_1^+$ states.[31]

### B. Negative-parity states

Figure 7 illustrates the population of negative-parity states in relation to states of the quasi-ground and quasi-$\gamma$ bands at an incident neutron energy of 2.5 MeV. Additional negative-parity states of high spin have been reported from reaction studies[47,48,61,62] and the decay[51,52] of the high-spin isomer of $^{194}$Ir. Bands of low-lying odd-parity states in the even mass Os, Pt, and Hg nuclei have been observed[47,61-63] to display a characteristic sequence of levels differing by two units of angular momentum with strong $E2$ transitions between successive levels. Clearly, these bands cannot be interpreted as octupole bands within a deformed strong-coupling framework. A summary of the known negative-parity yrast states of $^{194}$Pt is shown in Fig. 8(a).

On the suggestion[47] that these states are predominantly two-quasineutron configurations involving a low-$j$ ($3p_{1/2}$, $3p_{3/2}$, or $2f_{5/2}$) single-particle state coupled to a high-$j$ partner ($i_{13/2}$) or similar two-quasiproton configuration, Neergård *et al.*,[64] explored the Coriolis coupling between two-quasiparticle states in an axially symmetric oblate nucleus. For this system of two-quasiparticle states they demonstrated that the principal effect of the Coriolis force is the decoupling of the high-spin quasiparticle. This high-$j$ particle is weakly coupled to an effective rotor composed of the core and the strongly core-coupled low-spin quasiparticle. A band with $\Delta J = 1$ develops, where the lowest-energy states have angular momenta approximately equal to the spin of the decoupled particle. A short range residual interaction between the quasiparticle configurations separates the odd- and even-spin members of the band, so that the odd-spin states occur at lower energies to form an apparent $\Delta J = 2$ band.

While accounting for the negative-parity states of the Hg nuclei quite successfully, the semi-decoupled model of Neergård *et al.*,[64] did not reproduce the properties of the Pt nuclei. The most obvious shortcomings were that the $5^-$ states were predicted at energies which were too high and the large $7^-$ to $9^-$ gap was not predicted. Within the framework of the semi-decoupled model, Toki *et al.*,[65] generalized the calculations to include nonaxial deformations. Using a value of $\gamma = 30°$, as suggested by the comparison of the spectra of odd-mass nuclei with particle-core coupling calculations,[66-70] good agreement was obtained for the even-mass Pt nuclei. The introduced asymmetry increased the $7^-$ to $9^-$ energy separation, while a decrease in energy of the $5^-$ state in the Pt nuclei was partially due to smaller gap parameters and partially accounted for by the increased role of proton excitations in these nuclei as opposed to the Hg isotopes. The predicted level energies, forming even- and odd-spin yrast parabolas, and preferred decay paths are indicated in Fig. 8(b).

In $^{194}$Pt the most complete set of low- and high-spin odd parity states in this region has been identified, and the assignments are certain in most cases. We have contributed the proposed $4^-$ level at 1883.3 keV. It should be noted, however, that the angular distribution of the $4^- \to 3^-$ $\gamma$ ray shows a much larger dipole component than the other $\Delta J = 1$ (e.g., the $6^- \to 5^-$ and $2^- \to 3^-$) transitions between odd-parity states. Considering the success of the semi-decoupled band calculations for $^{194}$Pt

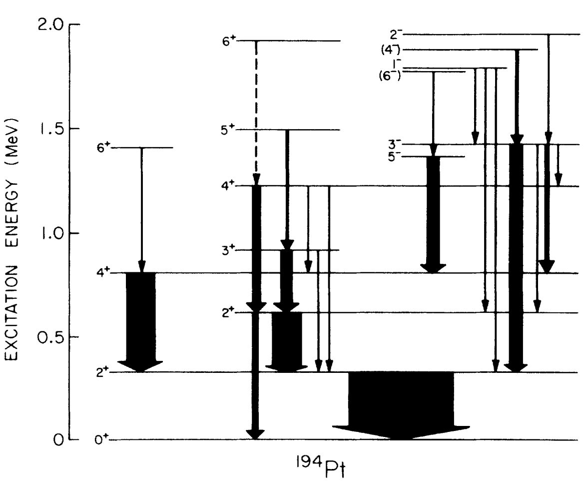


FIG. 7. Population of the quasi-ground, quasi-$\gamma$, and negative-parity bands in $^{194}$Pt at an incident neutron energy of 2.5 MeV. The arrow widths are proportional to the $\gamma$-ray intensity.

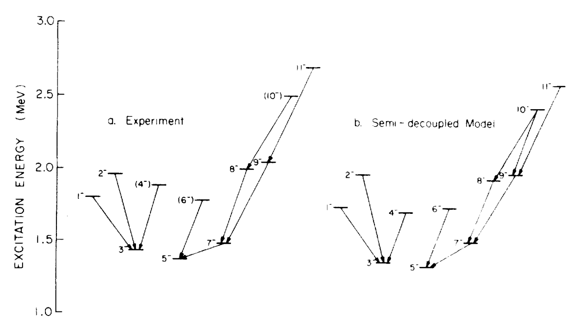


FIG. 8. Negative-parity states in $^{194}$Pt from (a) experiment and (b) the semi-decoupled model (Ref. 65). Transitions with the largest transition probabilities are shown. Uncertain spin assignments are shown in parentheses.

and other Pt nuclei,[47,61,62,71] the evidence for partially decoupled bands based on triaxial core excitations appears quite persuasive.

### C. $\gamma$ softness of the $^{194}$Pt core

Considerable controversy still exists as to the degree of $\gamma$ softness of the platinum nuclei. Baktash *et al.*,[5] have recently reviewed the evidence for softness and rigidity of these nuclei and have put forth arguments against rigid (or deep) potential energy surfaces. Indeed, good microscopic calculations (e.g., Refs. 10 and 72) in this region suggest that the potentials have no deep minima, and underlying both the IBM and BET calculations is a prediction of somewhat $\gamma$-unstable behavior for the Pt nuclei.

A considerable amount of data, however, appears to contradict the idea of softness in the $\gamma$ degree of freedom. The interpretation of the negative-parity states in $^{194}$Pt by the semi-decoupled model[64] relies on the assumption of a triaxial core.[65] Analysis of the unique-parity states of the odd-mass Pt and Au nuclei[73-77] within the triaxial-rotor-plus-particle model[66-70] gives values of $\gamma$, the asymmetry parameter, which are near 30°. The surprising constancy of $\gamma$ could suggest that these nuclei have stable triaxial shapes. Strong evidence for rigid shapes comes from the heavy-ion Coulomb excitation measurements of Lee *et al.*,[4] in $^{192}$Pt, $^{194}$Pt, and $^{196}$Pt. They compared experimental yields with various collective model calculations and concluded that a rigid-triaxial-rotor model calculation gave the best fit. Recent calculations by Baker[78] and Yadav *et al.*,[79] have employed the asymmetric rotor model to represent well the electromagnetic properties of heavy transitional nuclei. It may be, as suggested by the calculations of Girod and Grammaticos,[80] that these nuclei have nonzero dynamic mean values of $\gamma$, while remaining soft.

## V. CONCLUSIONS

Using detailed $\gamma$-ray excitation functions and angular distribution measurements from the $(n,n'\gamma)$ reaction, we have investigated the level structure of $^{194}$Pt. The decays of positive-parity states have been interpreted in terms of the IBM and BET models and are shown to be explained fairly satisfactorily by both approaches. An extensive set of negative-parity yrast states is well interpreted in the context of the semi-decoupled model.

Finally, our first examination of a nucleus in this region by low energy inelastic neutron scattering has demonstrated the power of these measurements, with states to $J=6$ being populated in an apparently nonselective manner. Such measurements and the development of systematics promise to add significantly to our knowledge of the structures of still other nuclei in this region.

## ACKNOWLEDGMENTS

We wish to thank Dr. R. F. Casten, Dr. J. A. Cizewski, Dr. P. J. Daly, Dr. P. T. Deason, Dr. R. M. Ronningen, Dr. T. Tamura, Dr. K. J. Weeks, and Dr. J. L. Wood for valuable discussions and exchanges. In particular, we thank Dr. Casten and Dr. Weeks for providing the IBM and BET calculations referred to in the text. We gratefully acknowledge Mr. B. Perraut for his cooperation during these experiments. This work was partially supported by the U. S. Department of Energy under Contract DE-AS05-79ER10365, the Research Corporation, and the National Science Foundation.

---

*Present address: Bell Laboratories, Allentown, Pennsylvania 18103.

†Present address: NL Petroleum Services, Box 1473, Houston, Texas 77001.

[1]A. Bohr, K. Dan. Vidensk. Selsk. Mat. Fys. Medd. 26, No. 14 (1952).

[2]A. Bohr and B. R. Mottelson, K. Dan. Vidensk. Selsk. Mat. Fys. Medd. 27, No. 16 (1953).

[3]G. Scharff-Goldhaber and J. Weneser, Phys. Rev. 98, 212 (1955).

[4]I. Y. Lee, D. Cline, P. A. Butler, R. M. Diamond, J. O. Newton, R. S. Simon, and F. S. Stephens, Phys. Rev. Lett. 39, 684 (1977).

[5]C. Baktash, J. X. Saladin, J. J. O'Brien, and J. G. Alessi, Phys. Rev. C 18, 131 (1978).

[6]A. S. Davydov and G. F. Filipov, Nucl. Phys. 8, 237 (1958).

[7]A. Faessler, W. Greiner, and R. K. Sheline, Nucl. Phys. 70, 33 (1965).

[8]L. Wilets and M. Jean, Phys. Rev. 102, 788 (1956).

[9]K. Kumar and M. Baranger, Phys. Rev. Lett. 17, 1146 (1966).

[10]K. Kumar and M. Baranger, Nucl. Phys. A122, 273 (1968).

[11]S. T. Belyaev, K. Dan. Vidensk. Selsk. Mat. Fys. Medd. 31, No. 11 (1959).

[12]L. S. Kisslinger and R. A. Sorenson, Rev. Mod. Phys. 35, 853 (1963).

[13]J. A. Cizewski, R. F. Casten, G. J. Smith, M. L. Stelts, W. R. Kane, H. G. Borner, and W. F. Davidson, Phys. Rev. Lett. 40, 167 (1978).

[14]F. Iachello and A. Arima, Phys. Lett. 53B, 309 (1974).

[15]A. Arima and F. Iachello, Phys. Lett. 57B, 39 (1975).

[16]A. Arima and F. Iachello, Phys. Rev. Lett. 35, 1069 (1975).

[17]A. Arima and F. Iachello, Ann. Phys. (N. Y.) 99, 253 (1976).

[18]A. Arima, T. Ohtsuka, F. Iachello, and I. Talmi, Phys. Lett. 66B, 205 (1979).

[19]T. Otsuka, A. Arima, F. Iachello, and I. Talmi, Phys.

Lett. 76B, 139 (1978).
[20]T. Otsuka, A. Arima, and F. Iachello, Nucl. Phys. A309, 1 (1978).
[21]A. Arima and F. Iachello, Phys. Rev. Lett. 40, 385 (1978).
[22]A. Arima and F. Iachello, Ann. Phys. (N. Y.) 111, 201 (1978).
[23]O. Scholten, F. Iachello, and A. Arima, Ann. Phys. (N. Y.) 115, 325 (1978).
[24]F. Iachello, G. Puddu, O. Scholten, A. Arima, and T. Otsuka, Phys. Lett. 89B, 1 (1979).
[25]A. Arima and F. Iachello, Ann. Phys. (N. Y.) 123, 468 (1979).
[26]R. F. Casten and J. A. Cizewski, Phys. Lett. 79B, 5 (1978).
[27]R. F. Casten and J. A. Cizewski, Nucl. Phys. A309, 477 (1978).
[28]T. Kishimoto and T. Tamura, Nucl. Phys. A192, 246 (1972).
[29]T. Kishimoto and T. Tamura, Nucl. Phys. A270, 317 (1976).
[30]T. Tamura, K. Weeks, and T. Kishimoto, Phys. Rev. C 20, 307 (1979).
[31]K. J. Weeks and T. Tamura, Phys. Rev. Lett. 44, 533 (1980).
[32]K. J. Weeks and T. Tamura, Phys. Rev. C 22, 1323 (1980).
[33]B. Harmatz, Nucl. Data Sheets 22, 433 (1977).
[34]M. C. Mirzaa, D. F. Coope, J. L. Weil, M. T. McEllistrem, A. J. Filo, and S. W. Yates (unpublished).
[35]M. T. McEllistrem, in ***Nuclear Research with Low Energy Accelerators,*** edited by J. B. Marion and D. M. Van Patter (Academic, New York, 1971), p. 359.
[36]M. T. McEllistrem, J. D. Brandenberger, K. Sinram, G. P. Glasgow, and K. C. Chung, Phys. Rev. C 9, 670 (1974).
[37]G. P. Glasgow, F. D. McDaniel, J. L. Weil, J. D. Brandenberger, and M. T. McEllistrem, Phys. Rev. C 18, 2520 (1978).
[38]*Table of Isotopes,* edited by C. M. Lederer and V. S. Shirley (Wiley, New York, 1978).
[39]A. D. Hanson and J. L. McKibben, Phys. Rev. 72, 673 (1947).
[40]J. T. Routti and S. G. Prussin, Nucl. Instrum. Methods 72, 125 (1969); J. T. Routti, University of California Lawrence Radiation Laboratory Report No. UCRL-19542, 2, 1969 (unpublished).
[41]S. D. Conte and C. de Boor, ***Elementary Numerical Analysis*** (McGraw-Hill, New York, 1972).
[42]D. E. Velkley, D. W. Glasgow, J. D. Brandenberger, and M. T. McEllistrem, Nucl. Instrum. Methods 129, 23 (1975) and J. W. Boring, Ph.D. dissertation, University of Kentucky, 1960 (unpublished).
[43]C. A. Engelbrecht, Nucl. Instrum. Methods 80, 187 (1970); 93, 105 (1971).
[44]V. J. Orphan, C. G. Hoot, and V. C. Rogers, Nucl. Sci. Eng. 40, 309 (1975).
[45]W. E. Kinney and F. G. Perey, Nucl. Sci. Eng. 63, 418 (1977).
[46]S. N. Tripathi, D. F. Coope, M. C. Schell, and M. T. McEllistrem, Phys. Rev. C (to be published).
[47]S. W. Yates, J. C. Cunnane, R. Hochel, and P. J. Daly, Nucl. Phys. A222, 301 (1974).
[48]S. A. Hjorth, A. Johnson, T. Lindblad, L. Funke, P. Kemnitz, and G. Winter, Nucl. Phys. A262, 328 (1976).
[49]P. J. Daly, private communication.
[50]E. Sheldon, J. A. Correia, D. R. Donati, and W. A. Schier, in ***Proceedings of the International Conference on the Interactions of Neutrons with Nuclei,*** edited by E. Sheldon, ERDA Report No. CONF-760715 P1, 1976, p. 1322.
[51]J. F. W. Jansen, H. Pauw, and C. J. Toeset, Nucl. Phys. A115, 321 (1968).
[52]H. Ton, G. H. Dulfer, J. Brasz, R. Kroondijk, and J. Blok, Nucl. Phys. A153, 129 (1970).
[53]G. D. Benson, A. V. Ramayya, R. G. Albridge, and G. D. O'Kelley, Nucl. Phys. A150, 311 (1970).
[54]J. Meyer-ter-Vehn, Phys. Lett. 84B, 10 (1979).
[55]P. T. Deason, C. H. King, T. L. Khoo, J. A. Nolen, and F. M. Bernthal, Phys. Rev. C 20, 927 (1979).
[56]J. A. Cizewski, E. R. Flynn, R. E. Brown, and J. W. Sunier, Phys. Lett. 88B, 207 (1979).
[57]J. E. Glenn, R. J. Pryor, and J. X. Saladin, Phys. Rev. 188, 1905 (1969).
[58]W. T. Milner, F. K. McGowan, R. L. Robinson, P. H. Stelson, and R. O. Sayer, Nucl. Phys. A177, 1 (1971).
[59]R. M. Ronningen, R. B. Piercey, A. V. Ramayya, J. H. Hamilton, S. Raman, P. H. Stelson, and W. K. Dagenhart, Phys. Rev. C 16, 571 (1977).
[60]J. K. Sprinkle, D. Cline, P. Russo, R. P. Scharenberg, and P. B. Vold, Bull. Am. Phys. Soc. 22, 545 (1977).
[61]M. Piiparinen, J. C. Cunnane, P. J. Daly, C. L. Dors, F. M. Bernthal, and T. L. Khoo, Phys. Rev. Lett. 34, 1110 (1975).
[62]L. Funke, P. Kemnitz, G. Winter, S. A. Hjorth, A. Johnson, and T. Lindblad, Phys. Lett. 55B, 436 (1975).
[63]H. Beuscher, W. F. Davidson, R. M. Lieder, A. Neskakis, and C. Mayer-Böricke, Phys. Rev. Lett. 32, 843 (1974).
[64]K. Neergård, P. Vogel, and M. Radomski, Nucl. Phys. A238, 199 (1975).
[65]H. Toki, K. Neergård, P. Vogel, and A. Faessler, Nucl. Phys. A279, 1 (1977).
[66]J. Meyer-ter-Vehn, Nucl. Phys. A249, 111 (1975).
[67]J. Meyer-ter-Vehn, Nucl. Phys. A249, 141 (1975).
[68]H. Toki and A. Faessler, Nucl. Phys. A253, 231 (1976).
[69]A. Faessler and H. Toki, Phys. Lett. 59B, 211 (1975).
[70]A. Faessler and H. Toki, Phys. Lett. 63B, 121 (1976).
[71]J. A. Cizewski, R. F. Casten, G. J. Smith, M. R. Macphail, M. L. Stelts, W. R. Kane, H. G. Borner, and W. F. Davidson, Nucl. Phys. A323, 349 (1979).
[72]U. Gotz, H. C. Pauli, K. Alder, and K. Junker, Nucl. Phys. A192, 1 (1972).
[73]J. Meyer-ter-Vehn, F. S. Stephens, and R. M. Diamond, Phys. Rev. Lett. 32, 1883 (1974).
[74]E. F. Zganjar *et al.*, Phys. Lett. 58B, 159 (1975).
[75]T. L. Khoo, F. M. Bernthal, C. L. Dors, M. Piiparinen, S. Saha, P. J. Daly, and J. Meyer-ter-Vehn, Phys. Lett. 60B, 341 (1976).
[76]S. K. Saha, M. Piiparinen, J. C. Cunnane, P. J. Daly, C. L. Dors, T. L. Khoo, and F. M. Bernthal, Phys. Rev. C 15, 94 (1977).
[77]C. Vieu, S. E. Larsson, G. Leander, I. Ragnarsson, W. De Wieclawik, and J. S. Dionisio, J. Phys. G 4, 531 (1978).
[78]F. T. Baker, Nucl. Phys. A331, 39 (1979).
[79]H. L. Yadav, A. Faessler, H. Toki, and B. Castel, Phys. Lett. 89B, 307 (1980).
[80]M. Girod and B. Grammaticos, Phys. Rev. Lett. 40, 361 (1978).